CANOPY PRUNING GRADE CLASSIFICATION BASED ON FAST FOURIER TRANSFORM AND ARTIFICIAL NEURAL NETWORK

Y. Shao, L. Tan, B. Zeng, Q. Zhang

ABSTRACT. *Canopy architecture optimization and pruning management are agricultural operations crucial for plant growth and fruit production. Classifying pruning grade and optimizing the tree canopy accordingly are essential for these operations. If the work is done properly, it can result in higher yields of quality fruit. In this article, we present a method utilizing fast Fourier transform (FFT) and a back-propagation artificial neural network (BP-ANN) to classify different pruning grades in cherry orchards with an upright fruiting offshoots (UFO) training system to illustrate our approach. The approach was implemented automatically by first using a discrete FFT to extract frequency information from images of a cherry tree canopy and then applying a band filter to digitize the 2D FFT spectrum to a 1D array. A BP-ANN model was then used to classify the pruning grade of the trees. By combining image processing and ANN-based classification techniques, our approach was resilient to details, such as specific leaf shapes and leaf vein structure, and achieved an accuracy rate of over 80% in classifying pruning grades for UFO cherry trees with respect to human expert grading. Principal component analysis (PCA) was also applied to simplify the prediction model complexity while maintaining a similar prediction accuracy rate with a much less complicated input data set. Experimental results showed that our method could provide real-time classification of pruning grades for UFO cherry trees with reasonable prediction accuracy.*

Keywords. *Artificial neural network, Fast Fourier transform, Principal component analysis, Pruning grade classification, Pruning management.*

Proper canopy architecture can contribute to better light interception and distribution in orchards, and it is also important for producing higher yields of quality fruit. On a theoretical basis, maximum potential assimilation may be realized by a canopy that absorbs all incoming light (Wagenmakers, 1995). Fruit yield per unit ground area has been shown to be positively correlated with light interception (Palmer, 1989). Insufficient light interception and exposition may reduce fruit size and color (Robinson et al., 1991; Palmer et al., 1992). Light interception can be increased by higher-density planting, suitable tree canopy size and shape, and higher leaf area index (relation of leaf area to ground area under the tree canopy). Due to its impact on fruit production, pruning to optimize the tree canopy structure is one of the most crucial horticultural operations in orchards. Therefore, efficient and accurate classification of pruning grade is essential and serves a pre-condition for effective tree canopy management.

Traditionally, the structural and geometrical information of tree canopy is obtained by performing manual measurements on trees, which is both time-consuming and highly subjective, as it relies heavily on the individual's experience and skills. Moreover, such measurement sometimes also requires destructive sampling of leaves (Daughtry, 1990). To solve these problems, a few indirect approaches, such as those based on transmission of radiation through the canopy (Ross, 1981; Norman and Campbell, 1989) and those based on spectral reflectance (Pinter et al., 1985; Miller et al., 2003), have been proposed for rapid canopy architecture measurement. However, these studies were qualitative by design, with an emphasis on proving the feasibility of their strategies. Researchers have found that such techniques tend to reach saturation too quickly for crops at their growth stage and are less capable of functioning properly when dealing with differences in canopies (Scotford and Miller, 2004). The goal of our study was to address these issues in a quantitative manner by developing a novel, efficient, and non-destructive method to provide real-time classification of pruning grades for cherry trees in an upright fruiting offshoots (UFO) training system using an integrated method that combines fast Fourier transform (FFT), artificial neural networks (ANN), and principal component analysis (PCA).

FFT is an efficient method to compute the discrete Fourier transform and the corresponding inverse form. FFT has been widely used in many applications, such as digital sig-

Submitted for review in September 2012 as manuscript number IET 9930; approved for publication by the Information & Electrical Technologies Division of ASABE in April 2014.

Any opinions, findings, and conclusions expressed in this article are those of the authors and do not necessarily reflect the views of the USDA, Washington State University, and Zhejiang University.

The authors are **Yongni Shao,** Lecturer, College of Biosystems Engineering and Food Science, Zhejiang University, Hangzhou, China; **Bolong Zeng,** Doctoral Student, School of Electrical Engineering and Computer Science, Washington State University, Richland, Washington; **Qin Zhang, ASABE Fellow,** Professor and Director, Center for Precision and Automated Agricultural Systems, Washington State University, Prosser, Washington; **Li Tan,** Assistant Professor, School of Electrical Engineering and Computer Science, Washington State University, Richland, Washington. **Corresponding author**: Li Tan, West 134L, WSU Tri-Cities, Richland, WA 99354; phone: 509-372-7167; e-mail: litan@wsu.edu.

Vol. 57(3): 963-971 ISSN 2151-0032 DOI 10.13031/trans.57.9930

nal processing, noise reduction, and image reconstruction (Nejati et al., 2008). In agricultural applications, Watchareeruetai et al. (2006) adopted FFT for detecting weeds in lawns. Nejati et al. (2008) used FFT to separate weeds from crops in real time. We use FFT to extract the spatial frequency spectrum from canopy images.

ANN refers to mathematical models that are intended to simulate the structural and/or functional aspects of biological neural networks in computer software (Huang et al., 2010). An ANN typically has an interconnected group of artificial neurons, and it processes information using a connectionist approach to computation (Baha'addin, 2013). Back-propagation neural network (BP-NN) is one of the most popular neural network topologies (He et al., 2007; Wu et al., 2008). It uses a learning process to minimize the global error of the system by modifying node weights, which are determined by the gradient descent rule (Wang et al., 2002). Yang et al. (2000) applied an ANN to recognize and classify crop and weeds, and the success rates for classifying corn plants and weeds were 100% and 80% respectively. Uno et al. (2005) used an ANN approach to develop corn yield prediction models, which showed greater prediction accuracy. Ushada et al. (2007) used an ANN model to describe the relationship between textural features and canopy parameters of Sunagoke moss.

PCA is a statistical technique to convert a set of possibly coupled variables into a set of linearly uncorrelated variables using an orthogonal transformation. Hence, it can be used as a prediction model to simplify the computational complexity. Uno et al. (2005) used PCA to reduce the number of input variables of their ANN. He and Ma (2010) modeled greenhouse air humidity using an ANN and PCA. They showed that the RMSE of stepwise regression was 4.5437, while the RMSE of the ANN based on PCA was 1.6745, which indicated that the results modeled by the ANN based on PCA were better than those obtained by stepwise regression. Mouazen et al. (2010) compared the measurement accuracy of soil properties for principal component regression (PCR), partial least squares regression (PLSR), and BP-ANN combined with PCA (PC-ANN). Their results showed that the PC-ANN modeling technique performed better than PCR and PLS.

Our intention was to develop an efficient method that can provide an accurate classification of pruning grades for cherry trees under the UFO training system by incorporating the aforementioned techniques. Several benefits could be obtained by doing so: (1) using FFT to process the images renders our approach resilient to details, such as the specific shapes of leaves, and is therefore highly extensible; (2) neural network is a widely used data mining tool, and its performance satisfies both the efficiency and accuracy requirements of this application; (3) finally, the PCA technique refines the inputs to the neural network model, thus minimizing the complexity of the prediction model and improving the efficiency without an observable drop in accuracy. These benefits also allow our approach to support real-time pruning grade classification, which renders it applicable in real-life field work.

The rest of this article is organized as follows. We first present the necessary information on the field study and pruning experiment that we conducted in cherry orchards, which provided the fundamental resources for our work. Next, we give an overview of the workflow of data processing, providing a detailed look into each building block with more specific information with respect to our particular application. Finally, we present the experiment results with a discussion of the performance of our method.

Field Experiment and Image Acquisition

Several different training systems are used for cherry trees. We selected an upright fruiting offshoots (UFO) training system (fig. 1) for our study. The UFO system has some advantages, such as the relatively simple structure, allowing easy access for orchard workers to perform field operations. Starting in the first year of growth, UFO trees usually go through a specific pruning procedure in the spring to form the tree canopy into a desirable pattern (Buler and Mika, 2009).

To obtain the data set for our experiment, we conducted manual pruning in August 2011 while measurements were performed between 4 and 5 August 2011 in a cherry orchard near Prosser, Washington. The data set includes

(a)

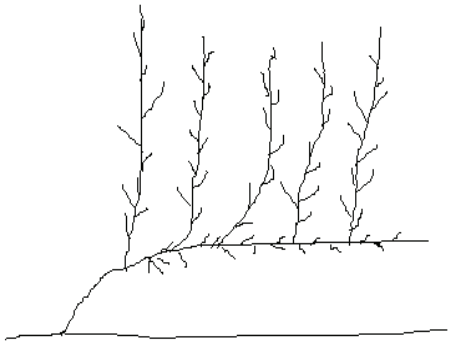

(b)

Figure 1. Upright fruiting offshoots (UFO) trained cherry trees: (a) photo of orchard and (b) typical branch pattern. These trees were used for pruning grade classification in this study.

100 cherry tree samples that were randomly selected in the orchard. Each of these manually pruned trees was given one of three pruning grades (over-pruning, premium pruning, and under-pruning) by an experienced horticulturist.

A color and infrared (CIR) camera (MS4100, Duncan Tech, San Diego, Cal.) was used to acquire images of the cherry trees. This camera consists of three CCD channels of green (G, 550 nm central band), red (R, 660 nm central band), and IR (NIR, 800 nm central band) and has a 25 mm focal length and 14.6° field of view. Each channel can capture a separate image with a pixel resolution of 1920×1080. To simplify the acquired images and block unnecessary visual noise, we used a white board as the background for all target trees during image acquisition. To minimize shadows on the white board, we acquired all images at noon. A 1320×1076 pixel region of interest (ROI) in the center of each acquired image was selected as the subject for analysis.

Data Processing and Pruning Grade Classification

With the images obtained from the orchard, an integrated data processing procedure was created for pruning grade classification. The FFT algorithms were implemented in Matlab 9.0 (The Mathworks, Inc., Natick, Mass.,), while we used DPS v3.01 (data processing system for practical statistics) to perform the BP-ANN classification. A total of 100 cherry tree images were taken from the cherry orchard. These images were used to validate the performance and accuracy of the developed pruning grade classification tool. Figure 2 shows the overall workflow of this procedure.

The first step in the procedure was using the discrete Fourier transform based image processing technique to extract the two-dimensional (2D) spatial frequency spectrum, which carried crucial canopy information, such as leaf coverage, from the acquired tree canopy images. We then used a digitizing algorithm on the spectrum and transform it into a one-dimensional (1D) array. The array was then fed to the BP-ANN model to identify the spectrum patterns representing different pruning grades. The BP-ANN model outputs the confidence level for the tree that was being evaluated and classified it into one of the three predefined grades. As a performance-enhancing option, a PCA processor was applied to extract the most informative components from the original spectrum data. PCA reduced the total number of inputs from 20 to 2 for the ANN model, thus accelerating the analysis process. This integrated ANN model with the PCA processor was called the PC-ANN identifier. We then compared the performances of the PC-ANN identifier and the BP-ANN model based on their classification accuracies and computation time using the same samples acquired from the orchard.

Fast Fourier Transform and Band Filtering

A set of FFT equations described by Gonzalez and Woods (2002) was used in this study. Let $f(x,y)$, for $x = 0, 1, 2,\ldots, M-1$ and $y = 0, 1, 2,\ldots, N-1$, denote an $M \times N$ image. The 2D discrete Fourier transform (DFT) of f, denoted by $F(u,v)$, is given by the following equation:

$$F(u,v) = \sum_{x=0}^{M-1}\sum_{y=0}^{N-1} f(x,y)\exp\left[-j2\pi\left(\frac{ux}{M}+\frac{vy}{N}\right)\right] \quad (1)$$

where $u = 0, 1, 2,\ldots, M-1$ and $v = 0, 1, 2,\ldots, N-1$. We used j to denote the imaginary unit to avoid confusion in this article.

The frequency domain of this equation is simply the coordinate system spanned by $F(u,v)$ with u and v as frequency variables. Let $R(u,v)$ and $I(u,v)$ represent the real and imaginary components of $F(u,v)$; the Fourier spectrum could then be defined as follows:

$$|F(u,v)| = \sqrt{R^2(u,v) + I^2(u,v)} \quad (2)$$

The phase angle of the transform is defined as:

$$\varphi(u,v) = \text{arctg}\left[\frac{I(u,v)}{R(u,v)}\right] \quad (3)$$

The power spectrum is defined as the square of the magnitude:

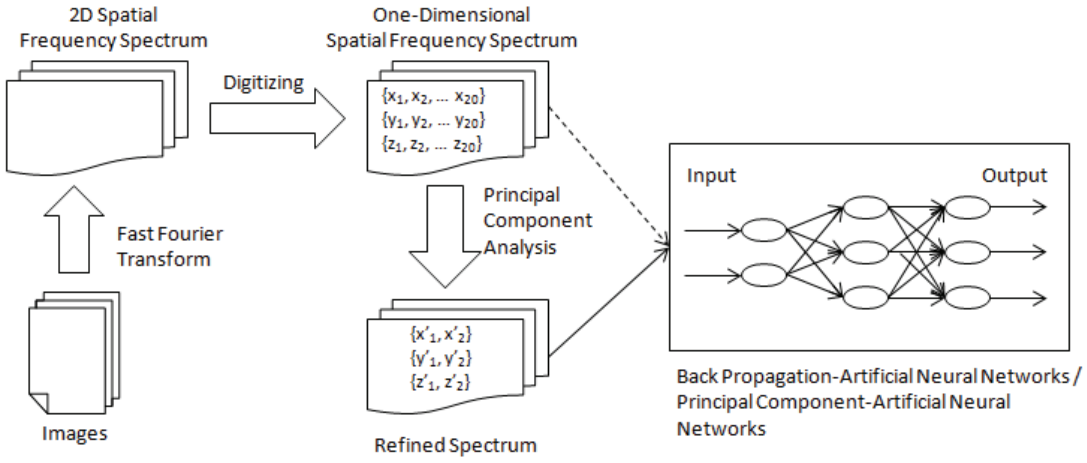

Figure 2. Workflow of the data processing procedure developed for tree pruning grade classification.

$$P(u,v) = \left|F(u,v)\right|^2 = R^2(u,v) + I^2(u,v) \quad (4)$$

The ROI of each cherry tree image was transformed to the frequency domain using 2D FFT analysis. We then applied the FFT shift function to move the zero-frequency component to the center of the image so that we could apply a band filter to it in the next step.

By transforming the original canopy images into spectrum data, we were able to maintain the essential canopy information in a uniform format for further analysis. In this way, the FFT-based image processing method was resilient to the specific shapes of the leaf and vein structures of the cherry trees. Consequently, our approach could be extended to other fruit tree systems.

For the next step, a digitization process using a band filter was performed on the obtained 2D FFT spectrum to transform it into a 1D array. We divided the image into 20 concentric circular bands in this process. First, we selected the biggest radius for these bands so that most of the information could be included. In our study, the radius was set to a value that allowed 99% of the frequency information to be covered by the areas included in the circular bands. Assuming that the first (smallest) band's radius is R, the other bands' radii were set to $\sqrt{2}R$, $\sqrt{3}R$,…, $\sqrt{20}R$. By doing so, each concentric circular band had exactly the same area, which was πR^2. Finally, the power within each concentric circular band was calculated. Assuming that the image size was $P \times Q$, the center of the image was $(P/2, Q/2)$, and the total power within each concentric circular band should be:

$$Ei = \Sigma P(u,v) \quad (5)$$

where

$$R*i \le \sqrt{\left(u - \frac{P}{2}\right)^2 + \left(v - \frac{Q}{2}\right)^2} < R*(i+1)$$

$$i = 0, 1, 2, \ldots, 19$$

Figure 3 presents the overall workflow of image processing in our proposed methodology. The sample images first went through the FFT transformation and were converted into a 2D frequency domain image. We then digitized the obtained frequency domain image with the aforementioned band filter. The bar chart on the right of figure 3 represents the power within each of the 20 concentric circular bands. These values were placed into a 1D array, which served as the input value for the BP-ANN identification model described later.

Back-Propagation Artificial Neural Network

The BP-ANN model was developed in this research to provide an efficient approach to identify the patterns of interest in a massive set of multivariable raw data. In order to obtain an optimal set for training the model with wide coverage, sufficient accuracy, and quick convergence, the BP-ANN was trained using a training set containing sample cases of tree pruning grades in different presentations. The number of input and output nodes was set with respect to the parameters presented in the digitized 1D spectrum data array and the classified pruning grades. The number of hidden layers and nodes was determined through a trial-and-

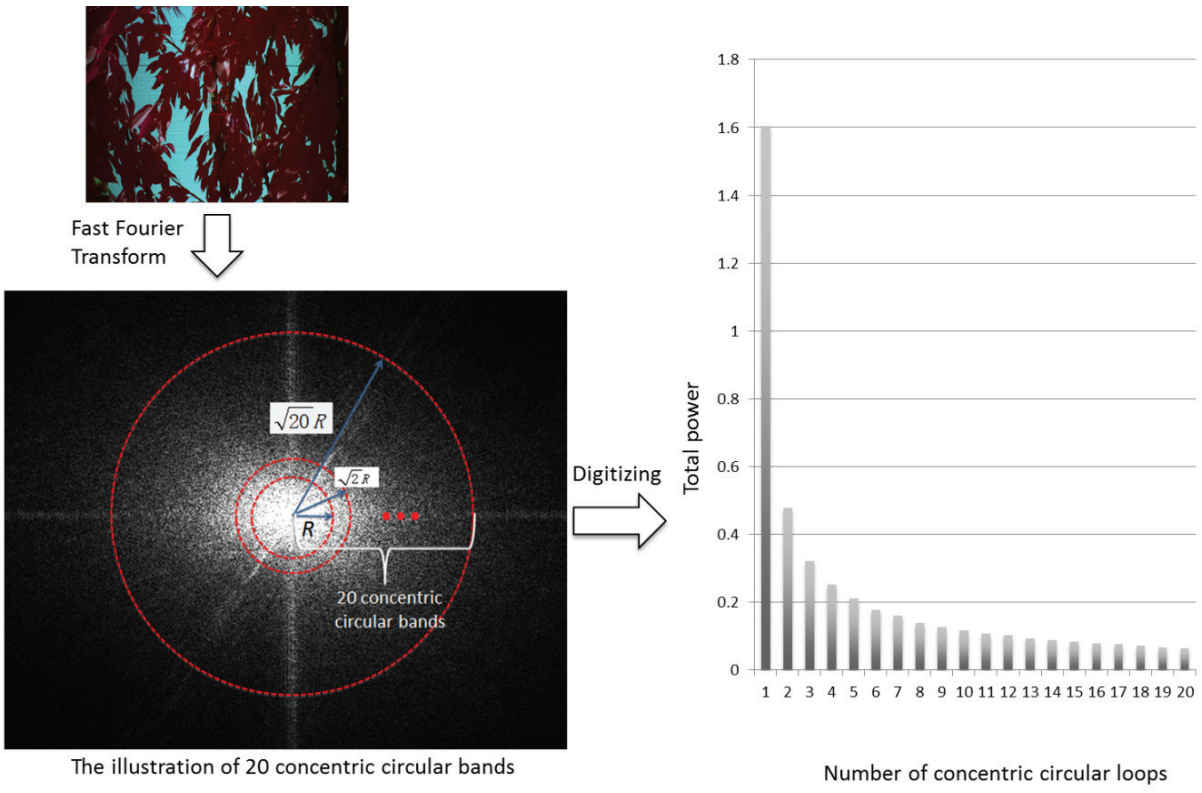

Figure 3. Overall workflow of image processing.

error approach in the training process. Full cross-validation and root mean square error (RMSE) were used to evaluate the performance of the BP-ANN model:

$$\mathrm{RMSE} = \sqrt{\frac{1}{n}\sum_{i=1}^{n}\left(\hat{y}_i - y_i\right)^2} \quad (6)$$

where n is the number of the observations in the prediction set, $\hat{y}_i$ is the prediction results of the neural network, and y_i is the three pruning grades of the cherry trees.

Because BP-ANN modeling is a very mature tool for data mining and pattern recognition, we intended to use this feature in our modeling approach to create high-speed pruning grade identification with high accuracy to support automatic real-time pruning classification.

The 100 samples were divided into two groups: 75 randomly chosen samples were used as the calibration set for training the BP-ANN model, and the remaining 25 samples were used for prediction. The training process was iterated until the algorithm achieved an acceptable (minimum) RMSE for the calibration model. The sigmoid function was applied as the transfer function, and the trainlm (Levenberg-Marquardt) function was used as the training function. As a practical matter, we chose a fixed upper bound to guarantee termination of the algorithm. In addition, we used RMSE as a performance-based parameter to avoid overfitting. Table 1 shows the RMSE values with different numbers of iterations during our experiment. In our experiment, the RMSE values reached the minimum at iteration 972 and remained steady thereafter. Furthermore, the RMSE values for calibration (RMSE-C) and validation (RMSE-V) were close to each other, at 0.35 and 0.38 respectively, indicating that the algorithm converged without overfitting. Based on this observation, we capped the maximal number of iterations at 1000 in this study, although the algorithm could still adapt itself and terminate earlier if the minimal RMSE value was achieved before reaching the set upper bound of iteration counts.

Through a multiple trial-and-error tuning process, the optimal structure of the BP-ANN model was set to one hidden layer with 12 nodes from an evaluated range of hidden layers between 5 and 15. We determined the range of the hidden layer based on the following formula (Jiao et al., 2009):

$$i = \sqrt{n+m} + a \quad (7)$$

where i is the number of neurons in hidden layers, n is the number of neurons in input layers, m is the number of neurons in output layers, and a is a constant from 1 to 10. Here n was 20 and m was 3, so the range of the hidden layer was 5 to 15 to the BP-ANN model.

In the calibration process, we realized that the learning rate and momentum terms had a substantial influence on the results. Because a large learning rate and momentum often cause an oscillation, an appropriate learning behavior should have a low learning rate and momentum. However, excessively small values for the learning rate and momentum will lead to a slow convergence. In our experiment, we concluded that when the learning rate was set within the range of 0.1 to 0.9 and momentum set within the range of 0.3 to 0.9, the BP-ANN model could reach an optimal learning rate of 0.1 and momentum of 0.9 when the training process ended.

Table 1. RMSE values of the calibration (RMSE-C) and validation (RMSE-V) models with different numbers of iterations.

	Iterations				
	800	900	972	1000	2000
RMSE-C	0.38	0.36	0.35	0.35	0.35
RMSE-V	0.40	0.39	0.38	0.38	0.38

Principal Component Analysis Processor

A principal component analysis (PCA) processor was applied to enhance the performance of the ANN model. Pruning grades were determined by making use of only the most informative components of the original spectrum data as the inputs for the ANN model. In this study, Unscrambler 9.7 (CAMO Software AS, Oslo, Norway) was used to perform the PCA analysis to obtain the optimized 1D digitized array. After PCA processing, some new uncorrelated variables, known as principal components (PCs), could be obtained. These PCs carried almost as much information of the original data as the original array, but the data set size was reduced or optimized to facilitate a post-processing procedure such as ANN. These PCs were then used as the inputs for the PC-ANN model. The following is the governing equation of PCA used in this study:

$$X = TP^{-1} + E \quad (8)$$

where X is an $N\times K$ data matrix, T is an $N\times A$ score vector matrix, P is a $K\times A$ loading vector matrix, E is an $N\times K$ residual matrix, N is the number of samples, K is the number of variables, and A is the number of PCs.

Results and Discussion

Pruning Grade Classification Based on BP-ANN Model

After the FFT analysis extracted 20 feature elements from each sample image, the ANN model used all 20 feature data (all being normalized) as its input variables. In addition, we defined a three-element integer-valued vector, with (0 0 1) representing over-pruning, (0 1 0) representing premium pruning, and (1 0 0) representing under-pruning, as classified by the expert horticulturist. Correspondingly, the output vector from the BP-ANN-based grade identifier was a three-element real-valued vector, with an element equal to or greater than 0.5 valued as checked and less than 0.5 valued as unchecked. For example, a vector of (0.10 0.30 0.60) denoted over-pruning, (0.30 0.60 0.10) denoted premium pruning, and (0.60 0.30 0.10) denoted under-pruning.

In this study, the inputs and outputs were scaled to [0, 1]. We identified a classification as correct if the deviation between the model's output value and the integer-value grade assigned by the expert horticulturist was less than 0.5; otherwise, the classification was considered incorrect. As shown in table 1, we determined that the lowest RMSE values could be achieved with 972 iterations, and the

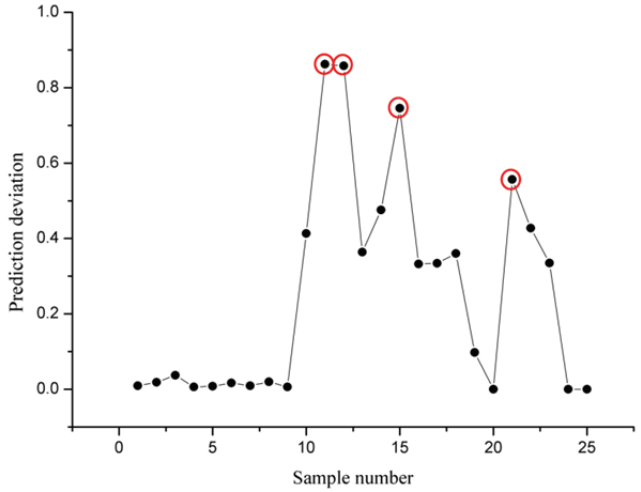

Figure 4. Deviations of 25 samples between model-assessed and expert-determined grades in the prediction test.

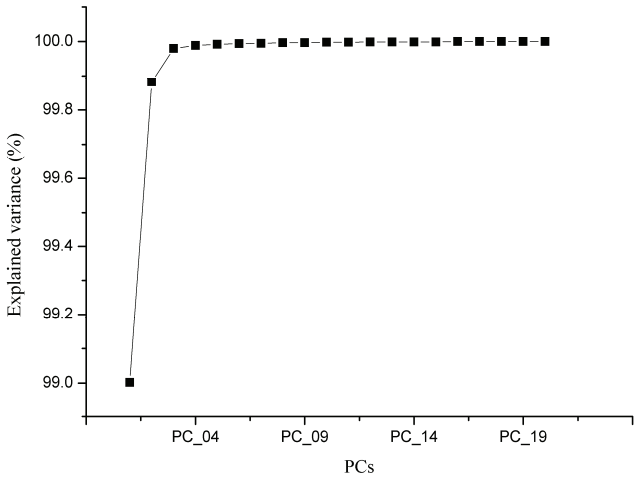

Figure 5. Explained variances of the 20 PCs.

RMSE values remained steady thereafter. The RMSE value reached 0.35 for the calibration model and 0.38 for the validation model, and the residual error of the calibration model was 6.214×10^{-5}. The RMSE values indicated 35% and 38% deviations, respectively, from the expert-assigned grades. Since both values were lower than the 0.5 threshold, the accuracy was acceptable enough for the model to be used for prediction.

Figure 4 shows the deviations in pruning grade classification for all 25 samples in the prediction test. The results showed that the deviations of 21 samples were lower than 0.5 (except samples 11, 12, 15, and 21, which are marked with red circles), which indicated that the model's assessment matched the expert's assessment. Overall, the RMSE value was 0.37 for the prediction process, which is close to RMSE-C and RMSE-V, and the accuracy rate of our approach reached 84%. After further analysis of the four unmatched samples, it was shown that two of these samples were very difficult even for the expert horticulturist to grade, and a "best guess" grading was assigned.

Pruning Grade Classification Based on PC-ANN Model

As introduced earlier, we also applied a PCA processor to enhance the data features and reduce the data dimensions for more effective analysis with the ANN model. PCA was performed on 20 digitized feature points of the 100 samples. These 20 feature points were used as the initial set of PCs, and the information that they captured served as the basis for subsequent analysis. The explained variances of the 20 PCs are presented in figure 5.

Figure 5 indicates that the first four PCs are sufficient to represent 99.9% of the original information from the image. Therefore, we built an ANN prediction model using only these four PCs. With the reduced size of the input set (the first four PCs) from the PCA analysis, the ANN structure was recalibrated to optimize the input nodes and hidden nodes. The new model was denoted the PC-ANN model to distinguish it from the previous model. To further reduce the input size, we tested the model by using only two and three PCs as well. After a multi-cycle calibration process, using the same sample set used for the BP-ANN model calibration, a new optimal topology was eventually found for the PC-ANN that consisted of only two input nodes (the first two PCs), four hidden nodes (the possible value being from 3 to 13), and three output nodes. Table 2 shows the input nodes (the first two PCs) for the 25 prediction samples.

The same 25 prediction samples were used to evaluate the performance of the PC-ANN model, which was compared with the BP-ANN model in terms of accuracy and processing time. Table 3 shows the pruning grade assessment results of the 25 prediction trees using the PC-ANN model. The results show that the PC-ANN model also correctly classified 21 out of the 25 samples, achieving the same accuracy rate of 84% as the BP-ANN model. For one sample (sample 16 in table 3), all the output grades were

Table 2. Input nodes for the 25 prediction samples based on the PC-ANN model.

Sample	Input Nodes				
No.	PC1	PC2	Expert Grading		
1	1.066	-0.14	1	0	0
2	0.596	-6.18E-02	1	0	0
3	0.343	-3.57E-02	1	0	0
4	1.352	-7.63E-02	1	0	0
5	1.026	-1.07E-02	1	0	0
6	0.534	-2.33E-02	1	0	0
7	0.925	-2.43E-02	1	0	0
8	0.497	-1.20E-02	1	0	0
9	2.141	-5.29E-02	1	0	0
10	-0.462	-4.23E-02	0	1	0
11	-0.314	7.66E-02	0	1	0
12	-0.282	5.64E-02	0	1	0
13	-0.256	-6.81E-02	0	1	0
14	-0.272	4.87E-02	0	1	0
15	-0.275	2.03E-03	0	1	0
16	-0.342	2.78E-02	0	1	0
17	-0.521	7.30E-02	0	1	0
18	-0.615	1.84E-02	0	0	1
19	-0.758	3.28E-02	0	0	1
20	-0.952	-7.13E-02	0	0	1
21	-0.558	7.15E-03	0	0	1
22	-0.61	3.49E-03	0	0	1
23	-0.483	-4.89E-02	0	0	1
24	-0.779	-6.31E-02	0	0	1
25	-1.037	-6.61E-02	0	0	1

Table 3. Pruning grade assessment results of 25 prediction trees using the improved PC-ANN model.

Sample No.	Output Vectors (Expert Grading)			Output Vectors (Model Grading)			Result
1	1	0	0	0.974	0.059	0.020	Match
2	1	0	0	0.962	0.064	0.027	Match
3	1	0	0	0.942	0.072	0.035	Match
4	1	0	0	0.982	0.054	0.014	Match
5	1	0	0	0.980	0.055	0.015	Match
6	1	0	0	0.964	0.064	0.024	Match
7	1	0	0	0.978	0.057	0.016	Match
8	1	0	0	0.963	0.066	0.024	Match
9	1	0	0	0.986	0.051	0.011	Match
10	0	1	0	0.019	0.211	0.612	Mismatch
11	0	1	0	0.051	0.682	0.025	Match
12	0	1	0	0.103	0.579	0.028	Match
13	0	1	0	0.287	0.127	0.335	Mismatch
14	0	1	0	0.129	0.528	0.031	Match
15	0	1	0	0.208	0.281	0.097	Mismatch
16[a]	0	1	0	0.066	0.459	0.078	Match
17	0	1	0	0.002	0.452	0.513	Mismatch
18	0	0	1	0.000	0.271	0.909	Match
19	0	0	1	0.000	0.044	0.999	Match
20	0	0	1	0.000	0.006	1.000	Match
21	0	0	1	0.001	0.339	0.719	Match
22	0	0	1	0.000	0.269	0.900	Match
23	0	0	1	0.013	0.197	0.707	Match
24	0	0	1	0.000	0.062	1.000	Match
25	0	0	1	0.000	0.001	1.000	Match

[a] All output grades are <0.5.

Table 4. Computation time comparison between BP-ANN and PC-ANN (values are in seconds; Class. indicates classification process).

Sample		BP-ANN Model		PC-ANN Model		
No.	FFT	Class.	Total	PCA	Class.	Total
1	4.809	0.289	5.098	0.080	0.139	5.028
2	4.687	0.154	4.841	0.043	0.111	4.841
3	4.645	0.156	4.781	0.049	0.133	4.827
4	4.662	0.187	4.849	0.047	0.169	4.878
5	5.126	0.152	5.268	0.060	0.128	5.314
6	4.969	0.250	5.219	0.054	0.150	5.173
7	4.645	0.277	4.922	0.073	0.156	4.874
8	4.558	0.206	4.764	0.038	0.142	4.738
9	4.898	0.221	5.119	0.052	0.150	5.100
10	4.898	0.146	5.044	0.037	0.132	5.067
11	4.643	0.199	4.842	0.061	0.146	4.850
12	4.573	0.158	4.731	0.056	0.142	4.771
13	4.908	0.153	5.031	0.045	0.127	5.080
14	5.070	0.174	5.244	0.050	0.130	5.250
15	4.772	0.272	5.044	0.069	0.168	5.009
16	4.694	0.220	4.914	0.068	0.150	4.912
17	5.012	0.199	5.211	0.056	0.152	5.220
18	4.666	0.183	4.849	0.059	0.146	4.871
19	4.716	0.168	4.874	0.067	0.144	4.940
20	4.718	0.196	4.914	0.076	0.147	4.941
21	4.977	0.295	5.272	0.083	0.160	5.220
22	4.801	0.276	5.077	0.060	0.155	5.016
23	4.854	0.287	5.141	0.055	0.150	5.059
24	5.030	0.258	5.288	0.047	0.137	5.214
25	4.940	0.201	5.141	0.042	0.144	5.126

less than 0.5. However, the grade for premium pruning was much higher than the other two. This could easily be resolved by introducing an additional assessment rule; hence, this example was considered a correct assessment as well.

The previous results showed that, given the size of our experimental data set, the PC-ANN model had an accuracy rate identical to that of the BP-ANN model. A noticeable advantage of the PC-ANN approach over the BP-ANN model is the reduction of the computation time needed for ANN classification. Table 4 lists the computation times for the different stages of the two approaches. Both approaches used the same FFT image transformation. For the BP-ANN model, the next step was using the neural network model to perform the classification. For the PC-ANN model, there was an extra step for PCA. All time values in table 4 are in seconds. Note that the classification times shown in the table do not include the calibration time, during which the neural network is being trained. We also omitted the time needed for the program to load in the images, since the cost of such operations varies greatly among different devices. In this study, all experiments were conducted on a MacBook Pro with a 2.2 GHz quad-core Intel Core i7 processor and 4 GB (two 2 GB SO-DIMMs) of 1333 MHz DDR3 memory.

As shown in table 4, the entire automated grading process could be completed in about 5 s, with the FFT image transformation accounting for about 94% of the overall computation time. As for the time needed for ANN classification, the PC-ANN model took less time than the BP-ANN model for all 25 samples, saving from 0.014 to 0.15 s. This improvement classification time ranged from 9% to 51.9%. For the PC-ANN model, there was an extra step for PCA processing before the classification. Therefore, the total processing time with the PC-ANN model may not always be shorter than with the BP-ANN model. Nevertheless, the PC-ANN method offered an advantage of needing less training time and smaller computer memory than the BP-ANN method because the PCA process reduced the number of inputs that the ANN had to process. This is a particularly desirable feature for mobile applications because a handheld device typically has limited computation power and memory compared with a desktop computer. Moreover, when used with a data set that is large in size and/or in dimension, the ANN classification process would take much longer than the PCA process. In that case, the PC-ANN model could be more efficient since it could reduce the time spent on classification. Our results indicated that the proposed workflow, shown in figure 2, may be used for real-time classifications of pruning grades in the field.

CONCLUSION AND FUTURE WORK

In this study, we presented a novel approach to minimize the feature data needed for an ANN grading model to automatically classify cherry tree pruning grades as over-pruning, premium pruning, and under-pruning. This automated grading approach used a discrete FFT analyzer and a specifically designed digitizer to extract 20 feature frequency points from cherry canopy images captured in an orchard under natural light conditions. Next, a BP-ANN model with 20 inputs and three outputs was created and calibrated to perform automatic classification of pruning grades. Our approach achieved a matching rate of 84% compared to an expert horticulturist's judgment of 100 sample trees. Furthermore, the framework we proposed was also resilient to the specific leaf shape and the leaf vein structure, so that it could be easily extended to other fruit tree systems. In addition, by applying a PCA method on the

original 20 feature points obtained from the FFT analysis, we were able to extract the two most informational feature points and develop an improved ANN identifier (the PC-ANN identifier). The PC-ANN identifier achieved improved performance by reducing the computation time needed for ANN classification while maintaining the same level of accuracy. The improvement in classification time ranged from 9.0% to 51.9%.

This work represents a significant step toward our long-term research goal of developing fully automated and efficient image classification algorithms for pruning specialty crops. The focus of this article is to introduce a novel image classification algorithm for pruning cherry trees in the UFO training system and to study its efficiency and feasibility. As an exploratory study, our experiment was limited to only 100 samples. We are prepared to conduct our follow-up study when a new pruning season comes along, so that we can further test the performance of our approach with additional data.

There are also several potential directions to explore in our future research. From the experimental results, we saw that FFT-based image processing accounted for the most of the time needed for the entire process. We used a software (Matlab) implementation of the discrete FFT algorithm in our experiment. Today, personal computing devices such as smart phones and tablet computers often incorporate purposely designed hardware for multimedia applications. These types of hardware may also be used to accelerate signal processing. For example, Wang et al. (2010) used the graphic processing unit (GPU) in a Motorola Droid phone to accelerate the FFT in their real-time face annotation application. A similar technique may be used to reduce the FFT processing time in our approach. Another future direction of our research is to provide a real-time and mobile solution for classifying pruning grade. Another possible improvement rests on refining the pruning grades. Instead of using a three-level grade system, we could provide the user with suggestions on how much the tree should be pruned or has been over-pruned. This would need more input from field experts, as well as building a model with respect to more information. Our work is capable of serving as a basis for such further research directions.

ACKNOWLEDGEMENTS

The research presented in this article was supported by the USDA Special Crop Research Initiative (SCRI) Program (SCRI-USDA-NIFA No. 2012-01213), the USDA Hatch Funds (WNP0745 and WPN00728), and the Agricultural Research Center (ARC) of Washington State University.

REFERENCES

Baha'addin, F. B. (2013). Kurdistan engineering colleges and using of artificial neural network for knowledge representation in learning process. *Intl. J. Eng. and Innovative Tech.*, *3*(6), 292-300.

Buler, Z., & Mika, A. (2009). The influence of canopy architecture on light interception and distribution in 'Sampion' apple trees. *J. Fruit and Ornamental Plant Res., 17*(2), 45-52.

Daughtry, C. S. T. (1990). Direct measurements of canopy structure. *Remote Sensing Rev., 5*(1), 45-60. http://dx.doi.org/10.1080/02757259009532121.

Gonzalez, R. C., & Woods, R. E. (2002). *Digital Image Processing* (2nd ed.). Englewood Cliffs, N.J.: Prentice Hall.

He, F., & Ma, C. W. (2010). Modeling greenhouse air humidity by means of artificial neural network and principal component analysis. *Computers Electr. Agric., 71*(supp. 1), S19-S23. http://dx.doi.org/10.1016/j.compag.2009.07.011.

He, Y., Li, X. L., & Deng, X. F. (2007). Discrimination of varieties of tea using near-infrared spectroscopy by principal component analysis and BP model. *J. Food Eng., 79*(4), 1238-1242.

Huang, J. S., Yasinsac, A., & Hayes, P. J. (2010). Knowledge sharing and reuse in digital forensics. In *Proc. 5th Intl. Workshop on Systematic Approaches to Digital Forensic Engineering (SADFE)* (pp. 73-78). Piscataway, N.J.: IEEE.

Jiao, S. H., Xia, B., Xu, H. J., & Liu, Y. (2009). The BP neural network prediction based on Matlab. *J. Harbin Senior Finance College, 1*, 55-56.

Miller, P. C., Scotford, I. M., & Walklate, P. J. (2003). Characterizing crop canopies to provide a basis for improved pesticide application. ASAE Paper 031094. St. Joseph, Mich.: ASAE.

Mouazen, A. M., Kuang, B., De Baerdemaeker, J., & Ramon, H. (2010). Comparison among principal component, partial least squares, and back-propagation neural network analyses for accuracy of measurement of selected soil properties with visible and near-infrared spectroscopy. *Geoderma, 158*(1-2), 23-31.

Nejati, H., Azimifar, Z., & Zamani, M. (2008). Using fast Fourier transform for weed detection in corn fields. In *Proc. Intl. Conf. Systems, Man, and Cybernetics* (pp. 1215-1219). Piscataway, N.J.: IEEE. http://dx.doi.org/10.1109/ICSMC.2008.4811448.

Norman, J. M., & Campbell, G. S. (1989). Canopy structure. In R. W. Pearcy, J. Ehleringer, H. A. Mooney, & P. W. Rundel (Eds.), *Plant Physiological Ecology: Field Methods and Instrumentation.* (pp. 301-325). New York, N.Y.: Chapman and Hall. http://dx.doi.org/10.1007/978-94-009-2221-1_14.

Palmer, J. W. (1989). The effects of row orientation, tree height, time of year, and latitude on light interception and distribution in model apple hedgerow canopies. *J. Hort. Sci., 64*(2), 137-145.

Palmer, J. W., Avery, D. J., & Wertheim, S. J. (1992). Effect of apple tree spacing and summer pruning on leaf area distribution and light interception. *Sci. Hort., 52*(4), 114-139. http://dx.doi.org/10.1016/0304-4238(92)90031-7.

Pinter Jr., P. J., Jackson, R. D., Ezra, C. E., & Gausman, H. W. (1985). Sun-angle and canopy-architecture effects on the spectral reflectance of six wheat cultivars. *Intl. J. Remote Sensing, 6*(12), 1813-1825. http://dx.doi.org/10.1080/01431168508948330.

Robinson, T. L., Lakso, A. N., & Ren, Z. (1991). Modifying apple tree canopies for improved production efficiency. *HortSci, 26*(B), 1005-1012.

Ross, J. (1981). *The Radiation Regime and Architecture of Plant Stands.* The Hague, The Netherlands: Dr. W. Junk Publishers.

Scotford, I. M., & Miller, P. C. H. (2004). Estimating tiller density and leaf area index of winter wheat using spectral reflectance and ultrasonic sensing techniques. *Biosystems Eng., 89*(4), 395-408. http://dx.doi.org/10.1016/j.biosystemseng.2004.08.019.

Uno, Y., Prasher, S. O., Lacroix, R., Goel, P. K., Karimi, Y., Viau, A., & Patel, R. M. (2005). Artificial neural networks to predict corn yield from compact airborne spectrographic imager data. *Computers Electr. Agric., 47*(2), 149-161. http://dx.doi.org/10.1016/j.compag.2004.11.014.

Ushada, M., Murase, H., & Fukuda, H. (2007). Non-destructive sensing and its inverse model for canopy parameters using texture analysis and artificial neural network. *Computers Electr.*

Agric., 57(2), 149-165. http://dx.doi.org/10.1016/j.compag.2007.03.005.

Wagenmakers, P. S. (1995). Light relations in orchard systems. PhD diss. The Netherlands: Wageningen University.

Wang, D., Ram, M. S., & Dowell, F. E. (2002). Classification of damaged soybean seeds using near-infrared spectroscopy. *Trans. ASAE, 45*(6), 1943-1948. http://dx.doi.org/10.13031/2013.11410.

Wang, Y.-C., Pang, S., & Cheng, K.-T. (2010). A GPU-accelerated face annotation system for smartphones. In *Proc. Intl. Conf. Multimedia* (pp. 1667-1668). New York, N.Y.: ACM Press. http://dx.doi.org/10.1145/1873951.1874317.

Watchareeruetai, U., Takeuchi, Y., Matsumoto, T., Kudo, H., & Ohnishi, N. (2006). Computer vision based methods for detecting weeds in lawns. In *Proc. Conf. Cybernetics and Intelligent Systems* (pp. 1-6). Piscataway, N.J.: IEEE.

Wu, D., Feng, L., Zhang, C., & He, Y. (2008). Early detection of *Botrytis cinerea* on eggplant leaves based on visible and near-infrared spectroscopy. *Trans. ASABE, 51*(3), 1133-1139. http://dx.doi.org/10.13031/2013.24504.

Yang, C. C., Prasher, S. O., Landry, J. A., Ramaswamy, H. S., & Ditommaso, A. (2000). Application of artificial neural networks in image recognition and classification of crop and weeds. *Canadian Agric. Eng., 42*(3), 147-152.